In Vivo Performance of a Modified CSTi Dental Implant Coating

Brooks J. Story, PhD*/William R. Wagner, PhD**/David M. Gaisser, MS***/
Stephen D. Cook, PhD****/Angela M. Rust-Dawicki, MS*****

Cylindrical dental implants coated with cancellous structured titanium (CSTi) were studied in a dog model. CSTi-2-coated and hydroxyapatite-coated (HA) implants were placed in 8 mongrel dogs. The porosity of the CSTi-2 coating was 9% less than that of the previously studied CSTi-1, resulting in greatly improved mechanical strength and cosmetic appearance. A slightly lower level of bone ingrowth was observed for CSTi-2 than for CSTi-1. However, the in vivo attachment strength of the CSTi-2 coating was comparable both to CSTi-1 and to an HA-coated control after 8 weeks. Measured porosity is technique dependent; digital analysis of in vitro samples yielded higher porosity values than in vivo histology cross sections.
(INT J ORAL MAXILLOFAC IMPLANTS 1998;13:749–757)

Key words: bone ingrowth, dental implant, osseointegration, porous coating, porous titanium

Porous titanium coatings have received considerable attention in implant dentistry as an alternative to dense coatings, such as titanium plasma spray (TPS) and hydroxyapatite (HA).[1–6] Whereas HA and TPS coatings are designed to encourage a strong attachment to surrounding bone at the implant surface, porous coatings allow growth of bone into the porous regions of the coating. This ingrowth results in mechanical interlocking between the implant and the surrounding bone. Porous coatings have a well-established clinical history in orthopedics.[7–11] A dental implant coated with cancellous structured titanium (CSTi, Sulzer Calcitek, Carlsbad, CA) was shown to exhibit excellent osseointegration properties in a dog model.[12] Bone growth into the porous titanium coating was as high as 92% in the femur. Bone attachment strength was comparable to that of an HA-coated control, reaching values as high as 12 and 32 mPa after 34 weeks in the mandible and femur, respectively. Moreover, light microscopy indicated that no fibrous tissue was apposed to the coating. In a separate animal study, it was demonstrated that the CSTi coating was no more susceptible than an HA-coated control to infection spreading from the oral cavity.[13] The CSTi coating was thus determined to have excellent potential as an alternative to ceramic or metallic dental implant coatings.

Although the CSTi coating performed well in vivo, its in vitro mechanical strength was actually lower than that of HA. Specifically, the tensile strength of the porous coating was less than 2,500 psi (17 mPa), compared to over 4,000 psi (28 mPa) for typical plasma-sprayed HA coatings. It would be desirable to maximize the CSTi coating strength if its in vivo performance could be retained, since higher strength is potentially important in cases of extreme loading or trauma. In addition, a small fraction of the CSTi pores were large enough that they traversed the entire thickness of the coating. Although these large pores did not compromise the effectiveness of the implants, they were determined to be cosmetically undesirable. This paper reports on a reformulated

*Project Manager, Advanced Materials, Sulzer Calcitek, Carlsbad, California.
**Vice President, Research and Development, Sulzer Calcitek, Carlsbad, California.
***Research Scientist, US Biomaterials Corporation, Alachua, Florida.
****Lee C. Schlesinger Professor, Tulane University School of Medicine, Department of Orthopedic Surgery, New Orleans, Louisiana.
*****Research Scientist, Tulane University School of Medicine, Department of Orthopedic Surgery, New Orleans, Louisiana.

Reprint requests: *Dr Brooks J. Story, Sulzer Calcitek Inc, 2320 Faraday Avenue, Carlsbad, CA 92008. Fax: 760-431-7811.*

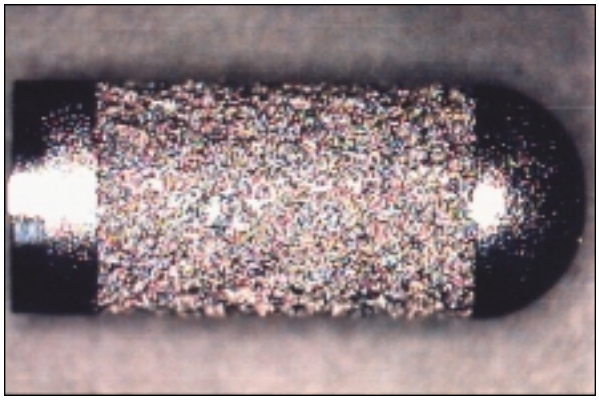

Fig 1 Cylindric implant with CSTi-2 coating.

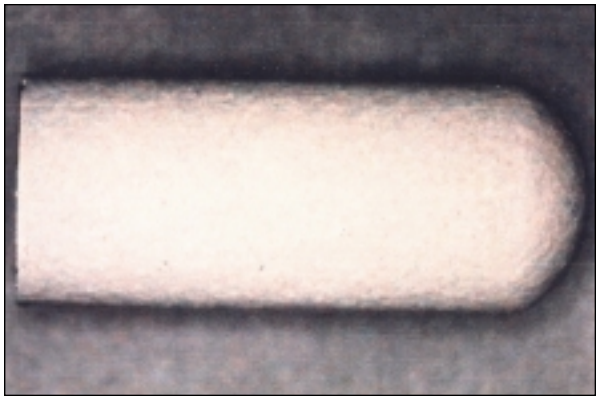

Fig 2 Control implant with hydroxyapatite coating.

CSTi coating that has a reduced porosity, which results in greater mechanical strength and a more desirable cosmetic appearance. For clarity, the original coating is designated here as CSTi-1 and the reformulated coating as CSTi-2. All data presented for CSTi-1 were taken from previous studies.[12,13]

Materials and Methods

CSTi Implants. Deposition of the CSTi coating onto the implants was performed by Sulzer Orthopedics (Austin, TX). CSTi implant bodies are composed of a titanium-aluminum-vanadium-ELI (Ti6-Al4V-ELI) alloy, and the porous coating is made of commercially pure titanium. All implants were 4.0 mm in diameter and 10.0 mm in length. As shown in Fig 1, the implant dimensions are similar to those of the Integral implant (Sulzer Calcitek), except that the Integral's apical vent holes have been eliminated. The CSTi implant features a machined interface ring 0.75 mm wide at its coronal end. Apical to this ring is a 0.75-mm-wide grit-blasted band, which was originally designed to encourage implant-bone attachment above the CSTi coating, thereby minimizing the potential for exposure of the porous coating to the oral cavity. The porous coating was deposited between the grit-blasted band and a point 2 mm from the apical hemispheric end, which was also grit blasted. The CSTi coating was 0.015 in (381 μm) thick.

HA Implants. Hydroxyapatite-coated Integral implants, 4.0 mm in diameter and 10.0 mm in length, without the apical vent holes featured on commercial devices were used as control samples. Hydroxyapatite coatings were deposited by plasma spraying under standard production conditions used by Sulzer Calcitek. The HA coating was applied to the entire surface of the implant and was 0.002 to 0.003 inches (50 to 75 μm) thick (Fig 2).

Animal Model. Eight adult mongrel dogs were used. The animals were selected on the basis of their availability, ease of handling, anatomical size, and bone repair and remodeling characteristics. All animals were 2 to 4 years old and were quarantined for 2 weeks prior to surgery to screen for acute or chronic medical conditions. Animals were designated using standard identification procedures. Animals were selected to ensure uniformity of size and weight so as to limit the variability of implant fit and bone quality. Presurgical radiographic screening was used to assure adequate femur and mandible size for implantation and to check for preexisting oral pathology.

All animal research was conducted at Tulane University School of Medicine. The study protocol was reviewed and approved by the university's Advisory Committee for Animal Resources. All experimentation was done in accordance with ethical and humane principles of research.

Experiment Design and Statistical Analysis. The CSTi-1 and CSTi-2 studies were designed so that only the CSTi formulation was varied. The 2 studies were conducted at the same time, by the same personnel, and at the same facilities. The HA-coated controls from both studies were identical, having been produced using the exact same process parameters for plasma spraying. This experimental design treats the individual implant as the appropriate experimental unit and allows direct comparisons between the CSTi-1 and CSTi-2 coatings.

Because the HA-coated controls from the 2 CSTi studies were identical, control data from the 2 studies were pooled. For example, the 4-week pullout data for HA-coated controls from the CSTi-1 study were pooled with the 4-week pullout data for HA-coated controls from the CSTi-2 study. This approach increased the overall number of control samples, thereby increasing the accuracy of the comparison between CSTi-1, CSTi-2, and HA-coated controls.

Six CSTi and 2 HA implants were placed in the mandible of each dog, for a total of 48 CSTi and 16 HA mandibular implants. Identical numbers of implants were placed in the femurs of each dog, for a total of 96 CSTi-2 and 32 HA implants in the study.

To test for statistically significant differences between the coatings, a standard *t* test was used to compare the pullout strength and bone ingrowth of CSTi-1 with those of CSTi-2 and to compare the pullout strength of CSTi-1 and CSTi-2 with that of HA-coated controls. In cases where normality or equal variance criteria were not met, a Mann-Whitney rank sum analysis was used to compare the populations. Statistical significance was defined as $P < .05$.

Surgical Procedures. Mandibular and femoral implant placement was performed 8 weeks after edentulation. Using standard aseptic techniques, surgery was performed under halothane gas anesthesia and was monitored by electrocardiogram and heart rate monitors. Extraction of the 4 mandibular premolars on both sides of the mandible was performed on all animals. An alveoloplasty was performed to remove surface irregularities and produce a smooth surface for subsequent implantation. Routine irrigation and closure with absorbable polyglactin sutures followed.

Implant Placement. Under general anesthesia, a mandibular crestal incision was made over the length of the extraction area and the alveolar ridge was exposed. A slow-speed, high-torque drill with internally irrigated bits was used to prepare 4 defects 4 mm in diameter on each side of the mandible. Each implant was then gently submerged 1 to 2 mm in bone. Routine irrigation, closure, and suturing followed. For femoral implantation, a lateral incision was made over the midshaft of the femur. Careful blunt dissection of the overlying tissues was performed to the lateral cortex of the femur. Four implant sites were prepared in each femur using procedures identical to the mandibular implantation method. Implants were tapped into place; routine irrigation and closure followed.

Animals received intramuscular antibiotics for 5 days postoperative and were placed on a soft-food diet for 2 weeks. Subcutaneous injection of torbutrol was used postoperative for pain control as necessary. Routine dental and femoral radiographs were taken immediately after surgery to ensure proper implant placement. After 3 to 5 days, animals were transferred from recovery cages to runs and allowed unrestricted motion.

Sacrifice. Animals were sacrificed using an intravenous barbiturate overdose (Beuthanasia-D, Schering-Plough, Madison, NJ). A gross pathologic examination of all implant sites was performed. All specimens were retrieved and placed in saline-soaked diapers, and radiographs were obtained.

Implant Retrieval. All nonessential soft tissues were removed from the mandible and femur specimens. Each implant site was isolated using a diamond saw. Following pullout testing, the CSTi-coated specimens were submitted for histology to determine the failure mechanism. All specimens were tested within 4 hours of sacrifice.

In Vivo Measurements. Attachment-strength measurements and histologic analyses were performed at 2, 4, 8, and 12 weeks postimplantation. Immediately after harvesting, the samples were pulled to failure on a closed-loop hydraulic test machine (MTS, Minneapolis, MN) operated in stroke control at a constant displacement rate of 2.0 mm per minute. Interface shear strength was determined by dividing failure load by the bone-implant contact area. Mandibular contact area was defined as the cylindrical area for control (HA-coated) implants and the area of porous coating for the CSTi implants. The calculated areas were 100.5 and 81.6 mm^2 for the HA and CSTi implants, respectively. Femoral cortical contact thickness was measured directly from contact radiographs of prepared specimens and was then used to calculate femoral implant contact area.

Histologic Analysis. The extent of bone ingrowth was determined immediately following mechanical testing using histology techniques described previously.[12,13] Specimens were fixed in 10% buffered formalin solution immediately following mechanical testing. Following fixation, the specimens were dehydrated in graduated (70% to 100%) ethyl alcohol solutions. The specimens were then placed in methylmethacrylate monomer. Following polymerization, the samples were sawed axially using a high-speed, water-cooled sectioning saw (Bronwill, San Francisco, CA) into sections approximately 700 to 1,000 μm thick. These sections were then mounted on acrylic resin slides and ground to a thickness of 50 μm using a metallurgical grinding wheel, and microradiographs were made using standard techniques. Following microradiography, the sections were further ground to a thickness of approximately 35 μm and stained with basic fuchsin and toluidine blue. Histologic analysis of bone ingrowth and coating porosity was performed using an inverted microscope (Carl Zeiss, Oberkochen, Germany) with transmitted and reflected light in conjunction with OPTIMAS 4.1 image analysis software (Optimas Corporation, Edmonds, WA).

In Vitro Coating Tensile Strength. Tensile strength of porous coatings was measured on CSTi-coated Ti6-Al4V-ELI disks. The porous coating was deposited into a pocket 0.015 in (381 μm) deep. A

minimum of 5 samples was used for each coating. One end of a 0.625-in (15.9-mm) diameter stainless steel cylindrical bar was attached to the CSTi coating surface using FM-1000 film adhesive (Cytec Industries, West Paterson, NJ). The adhesive thickness was 0.005 in (0.127 mm). The adhesive was heat cured according to manufacturer specifications. The bar/disk assembly was placed under tensile load and pulled to failure using an MTS model 810 test system. The displacement rate was 0.05 in per minute. Tensile strength was then calculated by dividing the failure load by the normal area of the tensile bar, 0.307 in^2 (198 mm^2).

SEM Analysis of CSTi Coating. For examination of the coating surface, CSTi-coated disks were used as received. For analysis of the coating cross section, a CSTi-coated implant was potted in Sampl-Kwik acrylic resin (Buehler USA, Lake Bluff, IL) and sectioned axially. After polishing to 1200 grit with silicon carbide abrasive paper, the acrylic resin was removed by dissolution in acetone and then baked at 500°C for 1 hour. All scanning electron microscopy (SEM) samples were gold-coated to minimize charging from surface oxide formation.

Porosity of CSTi Coating. In addition to the porosity measurements taken on histology samples, porosity of the CSTi-2 coating was measured using digital analysis of SEM images of cross-sectioned coated disks as described above. Coated disks were sawed in half axially to expose a cross section of the porous coating. Each sample was then potted in Epo-Thin epoxy (Buehler), and the sectioned surface was polished to a final finish of 1200 grit using silicon carbide abrasive paper. SEM analysis was conducted at General Atomics, La Jolla, California.

SEM images were taken of the cross-sectioned samples at ×150; at this magnification, nonporous areas appeared large enough to be easily selected during the digital analysis. Backscatter SEM mode was used to maximize the contrast between the metallic portion of the coating and the potting compound, which filled the coating pores. (In backscatter SEM mode, the porous component, which is filled with acrylic, appears black, and the nonporous metallic particles appear light gray, such that the porous and nonporous components are easy to distinguish.) Ten nonoverlapping images were taken across the entire coated portion of each CSTi-coated disk. SEM images were stored digitally as tagged image format (TIF) files.

For each SEM image, SigmaScan Pro software (SPSS, Chicago, IL) was used to assign a single color to the nonporous component (blue) and a second color to the porous component (red). The software was then used to determine the total number of pixels that made up the blue and red areas. For each SEM image, these pixel densities were then used to calculate the fraction of cross-sectional area occupied by the porous component. Porosity was determined by averaging the cross-sectional porous fractions of all SEM images.

As a check of the digital analysis method, porosity was measured directly from thick cylindrical pellets of CSTi-2. The pellets were approximately 1 in (250 mm) in diameter and 0.5 in (120 mm) in height. Density of the material was determined by weighing each pellet and dividing by its bulk volume. Porosity α was then calculated as follows:

$$\alpha = 1 - \frac{w_p}{V_p \rho_{Ti}}$$

where w_p and V_p are the weight and volume of the pellet, respectively, and ρ_{Ti} is the density of titanium (4.6 g/mL).

Results

Surface and cross-sectional views of a CSTi-2 coating sample are shown in Figs 3 and 4. In the cross-sectional sample, the potting compound has been removed to show the interconnectivity and random shapes of the pores. The porosity of the CSTi-1 coating, as determined using digital image analysis of histology cross sections was 48.1% (± 15.69%), and the porosity of CSTi-2 was 43.8% (± 7.4%) (P = .000). The tensile strength of CSTi-1 was 16.1 mPa (± 1.4 mPa), and that of CSTi-2 was 31.7 mPa (± 1.0 mPa). Table 1 compares the porosity measurements for the CSTi-2 coating obtained using different methods. The in vivo bone attachment strengths of CSTi and HA implants are given in Figs 5 to 8. Bone ingrowth data are shown in Figs 9 and 10 and histologic cross sections in Figs 11 and 12. Tables 2 and 3 summarize the comparisons between CSTi-1, CSTi-2, and HA-coated controls for bone attachment strength and bone ingrowth to the porous coatings. Statistical P-values are also provided in Tables 2 and 3.

A total of 4 CSTi- and 3 HA-coated mandibular implants were loose at the time of sacrifice, so pullout measurements could not be conducted on these samples. All loose implants were observed at 2 weeks, except for 1 HA-coated implant, which was observed at 4 weeks. In all cases, no evidence of infection appeared at the crestal incision sites, and bone ingrowth was observed on the loose CSTi implants. Thus, these implants in the early stages of healing may have been loosened during implant retrieval.

No fibrous tissue was observed at any of the bone-implant interfaces. Bone ingrowth to CSTi-2 was

Table 1 Comparison of Porosity Measurements for CSTi-2 Coating

Method	Porosity (%) (mean ± SD)
Digital analysis of histologic cross sections	43.8 ± 7.35
Digital analysis of SEM cross sections	57.2 ± 5.63
Bulk pellet measurement	60.5 ± 0.56

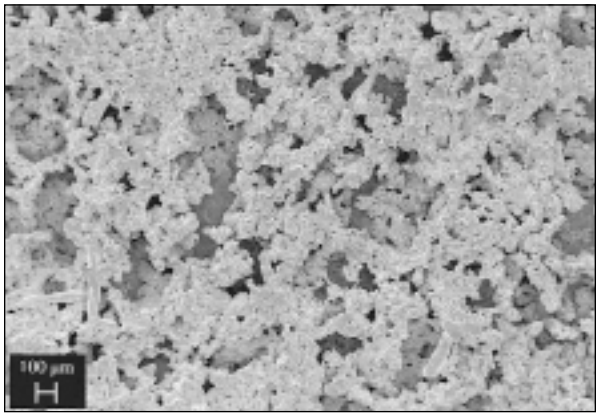

Fig 3 Surface of CSTi-2 coating.

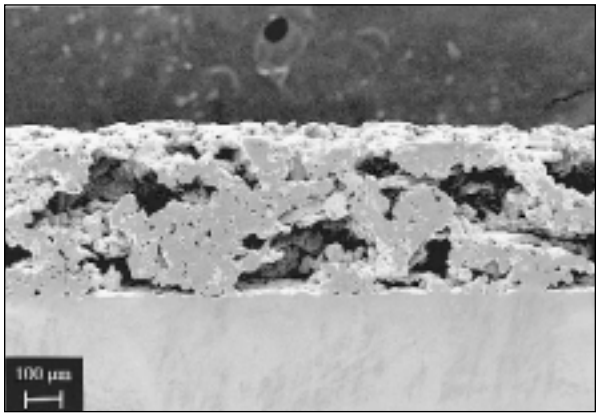

Fig 4 Cross section of CSTi-2 coating with potting compound removed.

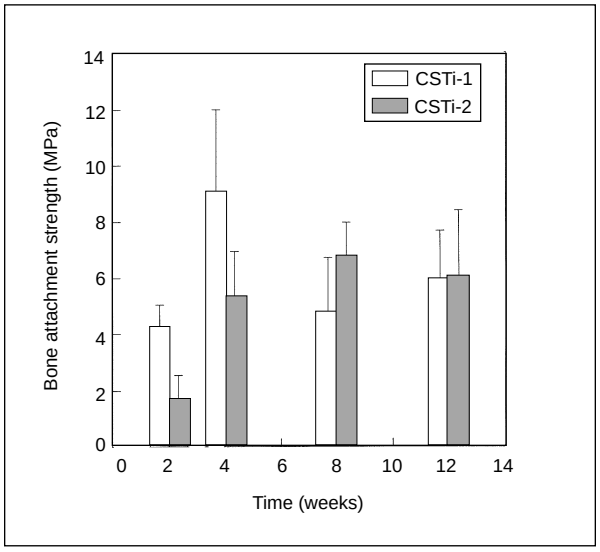

Fig 5 Bone attachment strength for CSTi-coated mandibular implants (mean ± SD).

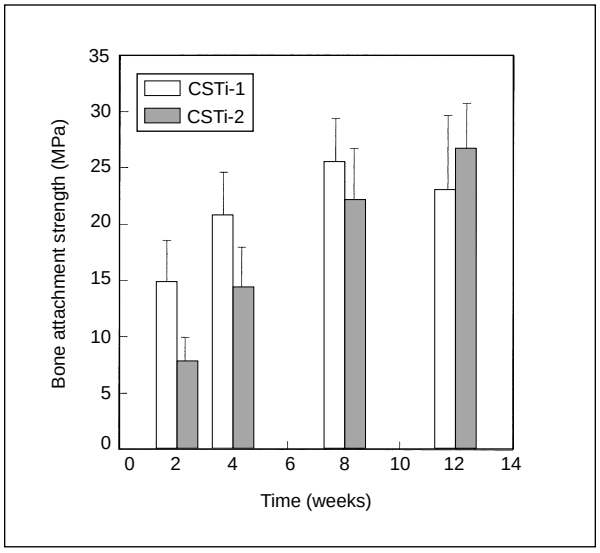

Fig 6 Bone attachment strength for CSTi-coated femoral implants (mean ± SD).

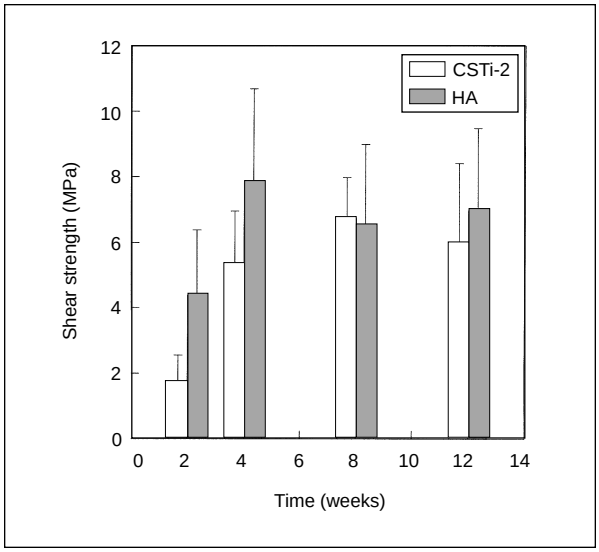

Fig 7 Bone attachment strength for CSTi-2- and HA-coated mandibular implants (mean ± SD).

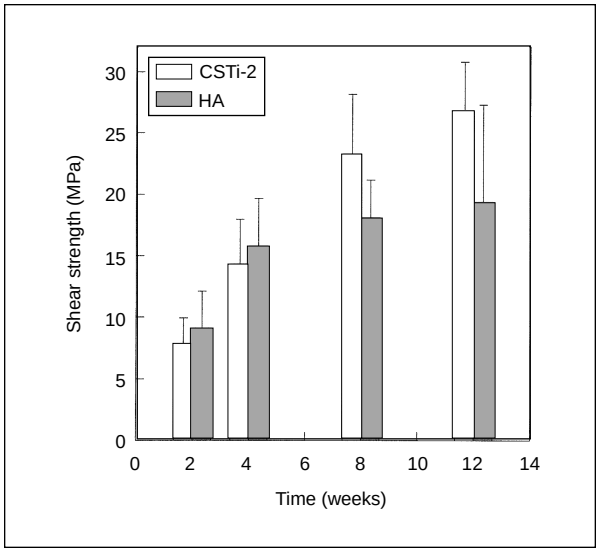

Fig 8 Bone attachment strength for CSTi-2- and HA-coated femoral implants (mean ± SD).

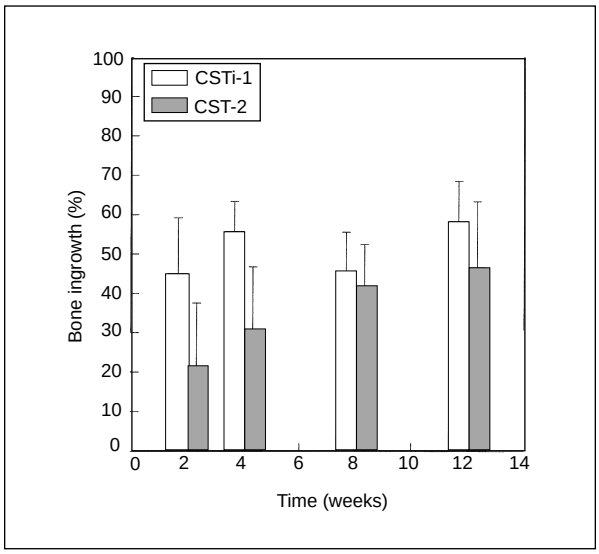

Fig 9 Bone ingrowth for CSTi-coated mandibular implants (mean ± SD).

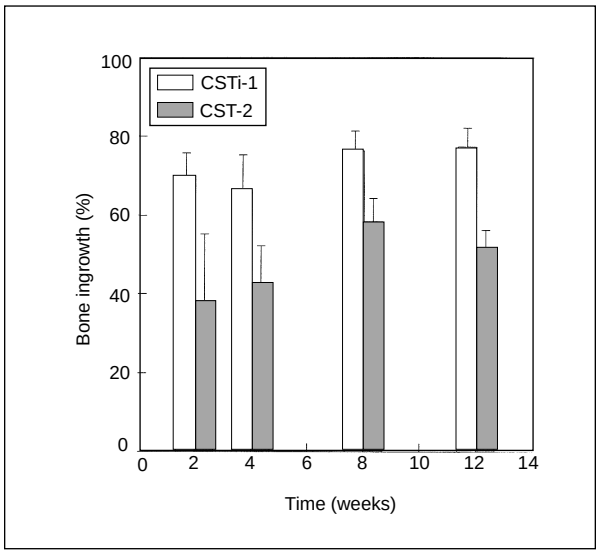

Fig 10 Bone ingrowth for CSTi-coated femoral implants (mean ± SD).

rapid; approximately 25% of the pore volume was filled after only 2 weeks in the mandible. As shown in Figs 11 and 12, bone ingrowth of more than 60% was observed in some areas of the coating at only 8 weeks. Bone ingrowth reached an average level of 46.5% at 12 weeks in the mandible and 51.4% at 12 weeks in the femur. At all time periods in the femur, CSTi-2 ingrowth was found to be less than that of CSTi-1 observed in the previous study, in which bony ingrowth averaged 58.2% at 12 weeks in the mandible and 76.2% at 12 weeks in the femur.[12] In the mandible, bone ingrowth to CSTi-1 and CSTi-2 was equivalent at 8 weeks.

In the mandible, CSTi-2 pullout strength was slightly less than that of HA at 2 weeks and 4 weeks. At 8 and 12 weeks, CSTi-2 was equivalent to HA. In the femur, pullout strength of CSTi-2 implants and HA-coated implants was equivalent at 2 and 4 weeks. At 8 weeks and 12 weeks, pullout strength of CSTi-2 implants was greater than that of HA implants. These

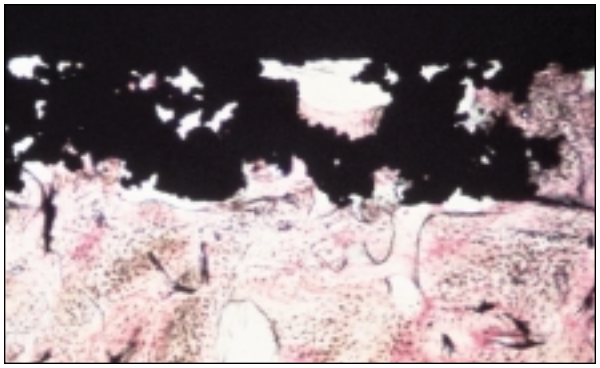

Fig 11 Ingrowth of bone to the CSTi-2 coating in the mandible at 8 weeks (original magnification ×20; basic fuchsin and toluidine blue).

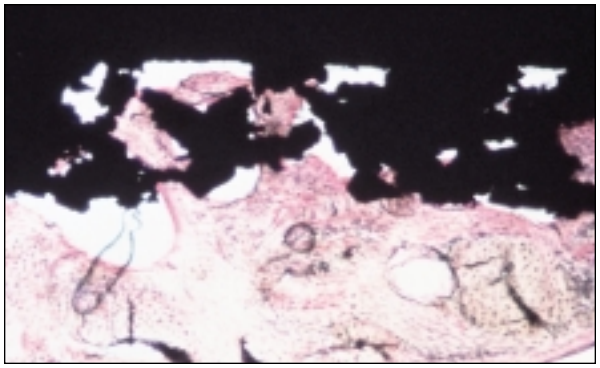

Fig 12 Ingrowth of bone to the CSTi-2 coating in the mandible at 12 weeks (original magnification ×20; basic fuchsin and toluidine blue).

Table 2 Pullout Strength Comparisons for CSTi-1-, CSTi-2-, and HA-coated Implants

	2 weeks		4 weeks		8 weeks		12 weeks	
Comparison	Mandible	Femur	Mandible	Femur	Mandible	Femur	Mandible	Femur
CSTi-1 vs HA	CSTi-1 = HA* (P = .9740)	CSTi-1 > HA* (P = .0031)	CSTi-1 = HA (P = .3140)	CSTi-1 > HA (P = .0047)	CSTi-1 = HA (P = .0531)	CSTi-1 > HA (P < .0001)	CSTi-1 = HA (P = .1619)	CSTi-1 = HA (P = .0755)
CSTi-2 vs HA	CSTi-2 < HA* (P = .0026)	CSTi-2 = HA (P = .2509)	CSTi-2 < HA (P = .0238)	CSTi-2 = HA (P = .3600)	CSTi-2 = HA (P = .8106)	CSTi-2 > HA (P = .0030)	CSTi-2 = HA (P = .3145)	CSTi-2 > HA* (P = .0000)
CSTi-1 vs CSTi-2	CSTi-1 > CSTi-2 (P < .0001)	CSTi-1 > CSTi-2 (P = .0001)	CSTi-1 > CSTi-2 (P = .0024)	CSTi-1 > CSTi-2 (P = .0011)	CSTi-1 < CSTi-2 (P = .0130)	CSTi-1 = CSTi-2 (P = .2394)	CSTi-1 = CSTi-2 (P = .9234)	CSTi-1 = CSTi-2* (P = .1300)

*Denotes Mann-Whitney rank sum test used instead of *t* test.

Table 3 Bone Ingrowth Comparisons for CSTi-1 and CSTi-2

Implant Location	2 weeks	4 weeks	8 weeks	12 weeks
Mandible	CSTi-1 > CSTi-2 (P = .0007)	CSTi-1 > CSTi-2 (P = .0010)	CSTi-1 = CSTi-2 (P = .5460)	CSTi-1 = CSTi-2 (P = .1223)
Femur	CSTi-1 > CSTi-2* (P = .0085)	CSTi-1 > CSTi-2 (P = .0012)	CSTi-1 > CSTi-2 (P = .0089)	CSTi-1 > CSTi-2 (P < .0001)

*Denotes Mann-Whitney rank sum test used instead of *t* test.

results compare favorably with the results obtained previously for CSTi-1.[12] Despite the greater degree of bony ingrowth for CSTi-1, attachment strength of CSTi-1 and CSTi-2 was equivalent at 8 weeks in both the mandible and femur.

Porosity values for CSTi-2, as determined using samples other than those from the histologic analyses, are presented in Table 1. The porosity values for in vitro samples are slightly higher than the values obtained from in vivo histology cross sections. Further, the in vitro samples yielded values much more consistent with bulk measurements taken on CSTi-2 pellets.

Discussion

Examination of the CSTi-2 coating surface and cross section shows that its pores are random in shape and orientation. The cross-sectional view of Fig 4 clearly shows the interconnectivity of the pores. Figure 4 also illustrates the continuous phase at the coating-substrate interface that results from sintering of the CSTi coating.

The porosity of CSTi-2 was significantly lower than that of CSTi-1 as measured in histology cross sections. Although the decrease in porosity was only about 9%, the in vitro coating adhesion strength of CSTi-2 was more than double that of CSTi-1.

It is interesting to note that porosity values varied with the type of cross section used for the analysis, as summarized in Table 1. In vitro samples, which were viewed using SEM, yielded higher porosity values than in vivo samples, which were viewed using light microscopy. This discrepancy may be explained by the method of sample viewing. In backscattered SEM images, only the outer surface of the cross-sectioned sample is observed. In effect, an infinitely thin, single plane of the cross section is observed. Histology cross sections in this study, however, are typically 35 to 50 μm thick. Since histology cross sections are illuminated from behind the sample, all of the titanium in the sample will appear black under a light microscope and will be interpreted as nonporous. In effect, the nonporous component from multiple planes of the sample will contribute to the nonporous component observed by the viewer. The fraction of titanium in a histology sample will thus appear artificially high, and the measured porosity in turn will be artificially low. The cross-sectional view of Fig 4 illustrates how the nonporous regions behind the plane of the cross section could contribute to the observed nonporous fraction of a thick sample illuminated from behind.

The accuracy of digital analysis using in vitro samples is supported by the direct measurements taken from CSTi-2 pellets. These values agree much more closely with those obtained using in vitro sample digital analysis. However, for purposes of comparing the relative porosities of CSTi-1 and CSTi-2, the use of histology cross sections should be valid, since the sample thicknesses were consistent in both studies.

Bone ingrowth was found to be lower in CSTi-2 compared to CSTi-1 at all time periods in the femur, and at 2 and 4 weeks in the mandible. The higher initial bone attachment strength of CSTi-1 is probably the result of this higher ingrowth in the early healing stages, which in turn is caused by a higher fraction of large pores. However, attachment strength data suggest that the long-term in vivo attachment strength is not significantly affected. This is supported by the observation that attachment failure in pullout tests was consistently observed at the bone-implant interface or within the bone itself. Neither cohesive failures of the CSTi coating nor substrate-CSTi adhesive failures occurred. Thus, the decrease in porosity and the resulting increase in coating strength did not affect the failure mode of CSTi implants. The increased mechanical strength of CSTi-2 may be beneficial in cases of extreme loading or trauma.

In the mandible, bone attachment strength of CSTi-2 implants was comparable to that of HA-coated controls at 8 and 12 weeks. In the femur, CSTi-2 attachment strength was equivalent to or greater than that of HA at all time periods. This is consistent with earlier research comparing CSTi-1 with HA-coated controls.[12]

Osseointegration has been defined as "a contact established between normal and remodeled bone and an implant surface without the interposition of nonbone or connective tissue, at the light microscopic level."[14] The lack of a fibrous tissue layer between surrounding bone and the CSTi coatings suggests that true osseointegration can be achieved using CSTi-coated dental implants. The results from the present study further demonstrate that bone ingrowth to CSTi coatings is an effective means of establishing a strong bone-implant interface that compares favorably with surface attachment to HA-coated implants.

Conclusions

A previously studied porous titanium coating (CSTi-1) was modified for improved mechanical strength and cosmetic appearance (CSTi-2). The 9% decrease in porosity did not significantly affect the bone attachment strength of CSTi-2 coated implants, although bone ingrowth was reduced. Bone ingrowth to the CSTi-2 coating averaged 46.5% in the mandible and 51.4% in the femur 12 weeks after placement. In the mandible and femur, bone attachment strength for the CSTi-2 coating was comparable to HA-coated controls in a dog model. By 8 weeks post-placement, the CSTi-1- and CSTi-2-coated implants were equivalent in pullout strength. The modified CSTi-2 coating provides a promising alternative to currently marketed dental implant coatings.

Acknowledgments

The authors are grateful to Bryan Mewhort and Chuck Wright of Sulzer Orthopedics, Inc, for deposition of the CSTi coatings.

References

1. Karagianes MT, Westerman RE, Hamilton AI, Adams HF, Wills RC. Investigation of long-term performance of porous-metal dental implants in nonhuman primates. J Oral Implantol 1982;10:189–207.
2. Young FA, Keller, JC. Porous titanium dental implants in primates and humans. Eng Med 1984;13:203–206.
3. Keller JC, Young FA, Natiella JR. Quantitative bone remodeling resulting from the use of porous dental implants. J Biomed Mater Res 1987;21:305–319.
4. Deporter DA, Watson PA, Pilliar RM, Melcher AH, Winslow J, Howley TP, et al. A histological assessment of the initial healing response adjacent to porous-coated, titanium alloy dental implants in dogs. J Dent Res 1986;65(8):1064–1070.
5. Deporter DA, Watson PA, Pilliar RM, Chipman ML, Valiquette N. A histological comparison in the dog of porous-coated vs. threaded dental implants. J Dent Res 1990;69(5):1138–1145.

6. Deporter DA, Watson PA, Pilliar RM, Pharoah M, Smith DC, Chipman M, et al. A prospective clinical study in humans of an endosseous dental implant partially covered with a powder-sintered coating: 3- to 4-year results. Int J Oral Maxillofac Implants 1996;11(1):87–95.
7. Bobyn JD, Pilliar RM, Cameron HU, Weatherly GC. The optimum pore size for the fixation of porous-surfaced metal implants by the ingrowth of bone. Clin Orthop Rel Res 1980;150:263–270.
8. Cook SD, Barrack RL, Thomas KA, Haddad RJ. Quantitative analysis of tissue growth into human porous total hip components. J Arthroplasty 1988;3:249–262.
9. Callaghan JJ. Current Concepts Review: The clinical results and basic science of total hip arthroplasty with porous-coated prostheses. J Bone Joint Surg [Am] 1993;75-A(2):299–310.
10. Hofmann AA, Murdock LE, Wyatt RWB, Alpert JP. Total knee arthroplasty: Two- to four-year experience using an asymmetric tibial tray and a deep trochlear-grooved femoral component. Clin Orthop Rel Res 1991;269:78–88.
11. Bloebaum RD, Rhodes DM, Rubman MH, Hofmann AA. Bilateral tibial components of different cementless designs and materials: Microradiographic, backscattered imaging and histologic analysis. Clin Orthop Rel Res 1991;268:179–187.
12. Cook SD, Rust-Dawicki AM, Story BJ, Gaisser DM, Wagner WR. In vivo evaluation of a CSTi dental implant: A healing time course study. J Oral Implantol 1995;XXI(3):182–190.
13. Cook SD, Rust-Dawicki AM, Story BJ, Gaisser DM, Wagner WR. In vivo evaluation of CSTi dental implants in the presence of ligature-induced peri-implantitis. J Oral Implantol 1995;XXI(3):191–200.
14. American Academy of Implant Dentistry. Oral Implantology Glossary of Terms. Implant Dent 1996;12:284.